ELSEVIER

Journal of Organometallic Chemistry 631 (2001) 87–93

Journal of Organometallic Chemistry

www.elsevier.com/locate/jorganchem

# Synthesis and structural characterization of $\{\mu_3\text{-H(Ph)C=C}\}FeCo_2(CO)_7dppm$ (dppm = $Ph_2PCH_2PPh_2$) and $\{\mu_3\text{-H(Ph)C=C}\}FeCo_2(CO)_{9-n}L_n$ [L = $PPh_3$ ($n = 1, 2$), $AsPh_3$ ($n = 1$)]

Quanling L. Suo [a,*], Hao Zhang [a], Yibin Wang [a], Li Wang [a], Linhong Wen [b], Xuebing Leng [b]

[a] *Chemical Engineering College, Inner Mongolia Polytechnic University, Hohhot 010062, China*
[b] *Institute of Elemento-organic Chemistry, Nankai University, Tianjin 300071, China*

Received 14 March 2001; received in revised form 30 May 2001; accepted 31 May 2001

**Abstract**

The new mixed-metal clusters $\{\mu_3\text{-H(Ph)C=C}\}FeCo_2(CO)_7dppm$ (dppm = $Ph_2PCH_2PPh_2$) (**1**) and $\{\mu_3\text{-H(Ph)C=C}\}FeCo_2(CO)_{9-n}L_n$ [L = $PPh_3$, $n = 1$ (**2**), $n = 2$ (**3**); $AsPh_3$, $n = 1$ (**4**)] have been synthesized by facile substitution reactions. The molecular structures of **1**, **2** and **4** have been determined by single-crystal X-ray analysis; dppm replaces two equatorial carbonyls from two $Co(CO)_3$ groups, and $PPh_3$ and $AsPh_3$ replace one equatorial carbonyl from a $Co(CO)_3$ group, respectively. The new compounds were characterized by IR, $^1H$-, $^{31}P$- (for **1**–**3**) NMR and MS. Cyclic voltammetric behavior for **1**, **2** and **4** was investigated, and the results show the order of σ-donator ability is CO < $PPh_3$ < $AsPh_3$ < dppm. 

*Keywords:* Mixed-metal clusters; Substitution reactions; Crystal structures

## 1. Introduction

The chemistry of transition metal carbonyl clusters has attracted a great deal of interest since 1970s [1–3]. Mixed-metal carbonyl clusters are currently under intensive investigation because of their potential catalytic applications [4]. Trinuclear clusters containing a $\mu_3$-vinylidene moiety could serve as model compounds in heterogeneous catalysis [5]; therefore, the study of substitution reactions on the clusters bearing a $\mu_3$-vinylidene moiety provides an opportunity to generate new catalysts for heterogeneous catalytic reactions. Although the kinetics and CO-exchange mechanism of substitution reactions of mixed-metal carbonyl clusters have been studied in some detail [6–9], there are few data on the replacement of CO by other ligands in mixed-metal carbonyl clusters bearing a $\mu_3$-vinylidene moiety. The parent cluster $\{\mu_3\text{-H(Ph)C=C}\}FeCo_2(CO)_9$ (**5**) was obtained by the reaction of $\{\mu\text{-PhC≡CHCo}_2(CO)_6\}$ with $Fe_3(CO)_{12}$ [10]. The substitution reactions of $\{\mu_3\text{-H(R)C=C}\}RuCo_2(CO)_9$ (R = H, Me, Ph) with $PMe_3$ and $PMe_2Ph$ [11] have been investigated, however, the reports on substitution reactions of the parent cluster **5** are relatively rare in the literature and only one example $\{\mu_3\text{-H(Ph)C=C}\}FeCo_2(CO)_7$-dppfe [dppfe = $(Ph_2PC_5H_4)_2Fe$] has been reported [12].

Although the interaction of the vinylidene (H(R)C=C) with the metal cluster core ($RuCo_2$ or $FeCo_2$) in mixed-metal carbonyl clusters bearing a $\mu_3$-vinylidene moiety has been described [10] studies on the effect of ligands on the interaction are very limited. The structural change of the cluster brought by the replacement of CO [13] is the main motivation to prepare the new substituted derivatives of the parent cluster **5**. The preparation and structural characterization of four new substituted derivatives have been described in this paper. The molecular structures of **1**, **2** and **4** were

* Corresponding author. Tel.: +86-471-6575837; fax: +86-471-6503298.
*E-mail address:* szj@mail.impu.edu.cn (Q.L. Suo).

0022-328X/01/$ - see front matter 
PII: S0022-328X(01)01020-8

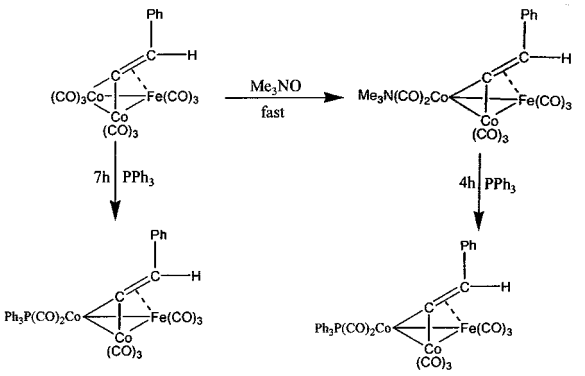


Scheme 1.

determined by X-ray diffraction. Their electrochemical properties were investigated by cyclic voltammetry.

## 2. Results and discussion

### 2.1. Synthesis and characterization of the new clusters

The reaction of the parent cluster **5** with dppm in toluene or L ligands in benzene at 75 °C in the presence of trimethyl-amine oxide ($Me_3NO$) gives the substituted derivatives $\{\mu_3\text{-H(Ph)C=C}\}FeCo_2(CO)_7$dppm and $\{\mu_3\text{-H(Ph)C=C}\}FeCo_2(CO)_{9-n}L_n$ [L = $PPh_3$ ($n = 1$, 2), $AsPh_3$ ($n = 1$)], respectively. The parent cluster **5** reacts with $PPh_3$ in benzene at 75 °C to give $\{\mu_3\text{-H(Ph)C=C}\}FeCo_2(CO)_8PPh_3$ in 36.1% yield in 4 h in the presence of $Me_3NO$ and in 27.1% yield in 7 h in the absence of $Me_3NO$ (see Scheme 1). This confirms that trimethylamine oxide plays a role as an oxygen transfer agent and accelerates the substitution reaction [14]. The cluster $\{\mu_3\text{-H(Ph)C=C}\}FeCo_2(CO)_8AsPh_3$ is a dark-green air-unstable solid, so its formation requires a longer reaction time(24 h). The IR spectra of these compounds indicate the characteristic absorption bands of the terminal carbonyl ligands in the region 2070–1912 $cm^{-1}$. The number of peaks in **3** is less than that of **2** in the IR spectra, indicating that the molecular structure of **3** has a greater degree of symmetry. In comparison with the IR spectra of the parent cluster **5** (2098, 2044, 1977 $cm^{-1}$), the CO absorption bands of the new clusters shift to low frequency consistent with the fact that dppm and the L ligands are stronger σ-electron donors and weaker π-electron acceptors than CO. The $^1$H-, $^{31}$P-NMR reflect that there are H(Ph)C=C, $PPh_3$, $AsPh_3$ and dppm ligands in new clusters, respectively. Cluster **1** is soluble in polar solvents such as THF, chloroform and toluene, and clusters **2**–**4** are soluble in both non-polar solvents such as hexane and polar solvents.

### 2.2. Electrochemical properties of clusters *1*, *2* and *4*

The electrochemical properties of clusters **1**, **2** and **4** have been studied by cyclic voltammetry at 298 K in a standard three-electrode system with $[NEt_4][ClO_4]$ in $CH_2Cl_2$ solution as the supporting electrolyte. The results are given in Table 1.

It can be seen from the electrochemical data that clusters **1**, **2** and **4** undergo a quasi-reversible single-electron oxidation at −0.76, −0.81 and −1.24 V, respectively, which is a slightly greater negative potential than that of their parent cluster **5**. This suggests that dppm, $PPh_3$ and $AsPh_3$ are stronger σ-electron donors. The fact that the $E_{1/2}$ for clusters **1**, **2** and **4** is more negative than that of their parent cluster **5** supports the fact that the order of σ-donor ability is $CO < PPh_3 < AsPh_3 <$ dppm. There are other irreversible oxidation peaks at $E_p = 1.14$ and 1.53 V (**5**), 0.97 V (**2**), 0.95 V (**4**), 0.81 and 1.45 V (**1**) while the irreversible oxidation site is on the cluster core $FeCo_2$ [15]. The first irreversible oxidation peak was assigned to forming $[\{\mu_3\text{-H(Ph)C=C}\}FeCo_2(CO)_{9-n}E]^+$ (E = $PPh_3$, $n = 1$; $AsPh_3$, $n = 1$; dppe, $n = 2$; no substituted

Table 1
Voltammetric data [a]

| Cluster | Reduction | | | | | | | | | |
|---|---|---|---|---|---|---|---|---|---|---|
| | First oxidation | | | | | | Second oxidation | | | |
| | $E_{pc}$ | $E_{pa}$ | $\Delta E$ | $E_{1/2}$ | $i_{pc} \times 10^6$ | $i_{pa} \times 10^6$ | $E_{pa}$ | $i_{pa} \times 10^5$ | $E_p$ | $i_{pa} \times 10^5$ |
| **1** | −1.35 | −1.24 | 112 | −1.30 | 7.87 | 3.59 | 0.81 | 1.50 | 1.45 | 0.56 |
| **2** | −0.91 | −0.76 | 146 | −0.84 | 2.85 | 1.58 | 0.97 | 0.65 | | |
| **4** | −0.99 | −0.81 | 188 | −0.90 | 6.46 | 3.67 | 0.95 | 1.72 | | |
| **5** | −0.84 | −0.73 | 106 | −0.79 | 5.08 | 5.50 | 1.14 | 2.39 | 1.53 | 1.93 |

[a] Platinum electrode ($Ag \mid Ag^+$ standard) with 0.001 M TEAP at 20 °C in 100 mV scan rate. $E_{pc}$=cathodic peak potential (V); $E_{pa}$ = anodic peak potential (V); $\Delta E = E_{pa} - E_{pc}$; $E_{1/2}$ = half-wave potential (V); $i_{pc}$ = cathodic peak current (A); $i_{pa}$ = anodic peak current (A).

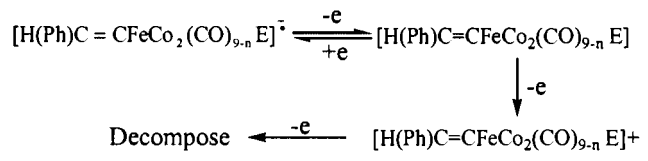


Scheme 2.

ligand E, $n = 0$) and the second (**1** and **5**) was considered to correspond to the decomposition of $[\{\mu_3\text{-}H(Ph)C{=}C\}FeCo_2(CO)_{9-n}E]^+$ [16] (see Scheme 2).

By comparison with the parent cluster **5** we can see that the cluster core ($FeCo_2$) reduction becomes more difficult and the cluster core oxidation becomes easier with the replacement of CO by $PPh_3$ or $AsPh_3$ or dppm. These facts can be interpreted to mean that the replacement of a CO ligand permits a greater accumulation of electron density on the cluster core leading to destabilization of the LUMO and in addition an increase in electron density on the cluster core raises the level of the HOMO to allow easy removal of an electron from the HOMO because these ligands are strong σ-electron donors and weak π-electron acceptors [17,18].

### 2.3. Molecular structures of clusters *1*, *2* and *4*

The molecular structures of the new clusters **1**, **2** and **4** were determined by X-ray single-crystal analysis. Crystal data and relevant structural parameters are enumerated in Table 2. The structures with the atom numbering schemes are shown in Figs. 1–3, and selected bond lengths and angles are listed in Tables 3–5, respectively.

Table 2
Crystal data and structure refinement parameters for **1**, **2** and **4**

| | **1** | **2** | **4** |
|---|---|---|---|
| Identification code | | | |
| Empirical formula | $C_{40}H_{28}Co_2FeO_7P_2$ | $C_{34}H_{21}Co_2FeO_8P$ | $C_{34}H_{21}AsCo_2FeO_8$ |
| Formula weight | 856.27 | 762.19 | 806.14 |
| Temperature (K) | 298(2) | 298(2) | 298(2) |
| Wavelength (Å) | 0.71073 | 0.71073 | 0.71073 |
| Crystal system | Monoclinic | Monoclinic | Triclinic |
| Space group | $P2_1/n$ | $P2_1/n$ | $P\bar{1}$ |
| Unit cell dimensions | | | |
| $a$ (Å) | 12.1979(9) | 15.8037(10) | 11.3272(9) |
| $b$ (Å) | 22.7600(18) | 11.4063(7) | 13.2113(10) |
| $c$ (Å) | 13.4119(10) | 19.0769(12) | 13.3605(11) |
| $\alpha$ (°) | 90 | 90 | 62.1710 |
| $\beta$ (°) | 95.203(2) | 106.6760(10) | 77.427(2) |
| $\gamma$ (°) | 90 | 90 | 66.825(2) |
| $V$ (Å$^3$) | 3708.1(5) | 3294.2(4) | 1624.0(2) |
| Z | 4 | 4 | 2 |
| $D_{calc}$ (Mg m$^{-3}$) | 1.534 | 1.537 | 1.649 |
| Absorption coefficient (mm$^{-1}$) | 1.406 | 1.528 | 2.512 |
| $F$(000) | 1736 | 1536 | 804 |
| Crystal size (mm) | $0.20 \times 0.15 \times 0.05$ | $0.45 \times 0.40 \times 0.05$ | $0.45 \times 0.30 \times 0.25$ |
| $\theta$ Range for data collection (°) | 1.77–25.02 | 1.48–26.41 | 1.73–26.39 |
| Index ranges | $-14 \le h \le 6$, $-27 \le k \le 26$, $-15 \le l \le 15$ | $-19 \le h \le 17$, $-14 \le k \le 12$, $-23 \le l \le 21$ | $-13 \le h \le 14$, $-11 \le k \le 16$, $-16 \le l \le 16$ |
| Reflections collected | 15 431 | 15 254 | 7734 |
| Independent reflections | 6549 ($R_{int} = 0.0539$) | 6728 ($R_{int} = 0.0358$) | 6573 ($R_{int} = 0.0220$) |
| Completeness to $\theta = 26.41°$ (%) | 100.0 | 99.6 | 98.7 |
| Max/min transmission | 0.9330, 0.7663 | 0.9275, 0.5464 | 0.5724, 0.3978 |
| Data/restraints/parameters | 6549/0/469 | 6728/2/497 | 6573/0/415 |
| Goodness-of-fit on $F^2$ | 0.991 | 1.035 | 1.126 |
| Final $R$ indices [$I > 2\sigma(I)$] | $R_1 = 0.0382$, $wR_2 = 0.0625$ | $R_1 = 0.0376$, $wR_2 = 0.0857$ | $R_1 = 0.0381$, $wR_2 = 0.0802$ |
| $R$ indices (all data) | $R_1 = 0.0856$, $wR_2 = 0.0737$ | $R_1 = 0.0706$, $wR_2 = 0.0993$ | $R_1 = 0.0588$, $wR_2 = 0.0878$ |
| Largest difference peak and hole (e Å$^{-3}$) | 0.383 and −0.334 | 0.699 and −0.302 | 0.466 and −0.583 |
| Weighting scheme | Calc. $w = 1/[\sigma^2(F_o^2) + (0.0218P)^2 + 0.0000P]$ where $P = (F_o^2 + 2F_c^2)/3$ | Calc. $w = 1/[\sigma^2(F_o^2) + (0.0458P)^2 + 0.0000P]$ where $P = (F_o^2 + 2F_c^2)/3$ | Calc. $w = 1/[\sigma^2(F_o^2) + (0.0356P)^2 + 0.0000P]$ where $P = (F_o^2 + 2F_c^2)/3$ |

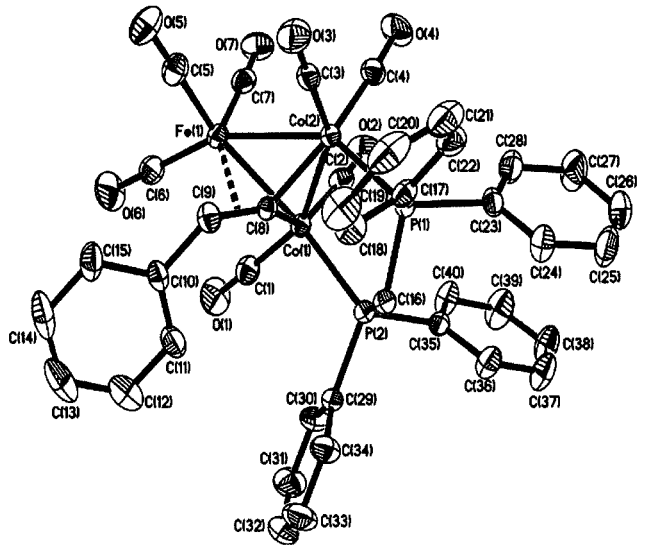


Fig. 1. Molecular structure of **1**.

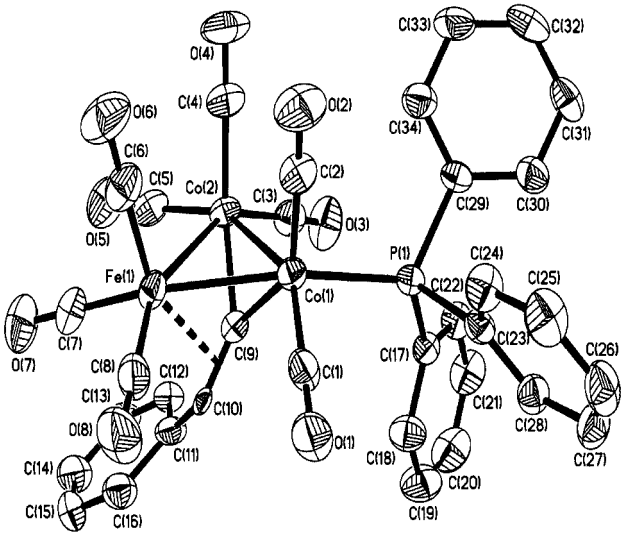


Fig. 2. Molecular structure of **2**.

The structures of the new clusters **1**, **2** and **4** are similar to that of the parent cluster **5** [12]. The crystal system and space group of **1** and **2** are monoclinic and $P2_1/n$, and that of **4** is triclinic and $P\bar{1}$ which is the same as that of the parent cluster **5**. The iron–vinylidene [>C(α)=C(β)H(Ph)] C(α) and C(β) bond lengths in **2** [Fe(1)–C(α), 1.947 Å and Fe(1)–C(β), 2.735 Å] are quite closer to those of the parent cluster **5** [1.94(2) and 2.63(3) Å]. The Fe(1)–C(α) (1.960 Å) and Fe(1)–C(β) (2.263 Å) bond lengths in **1** show that C(α) and C(β) atoms of the apical vinylidene [>C(α)=C(β)H(Ph)] group interact unequally with the Fe atom. It is interesting, however, that in **4** the Fe(1)–C(α) (2.024 Å) and Fe(1)–C(β) (2.072 Å) bond lengths are much more similar than in **1** and **2**. The Co(1)–C(α) (1.995 Å) and Co(1)–C(β) (2.1353 Å) bond lengths show there exists a

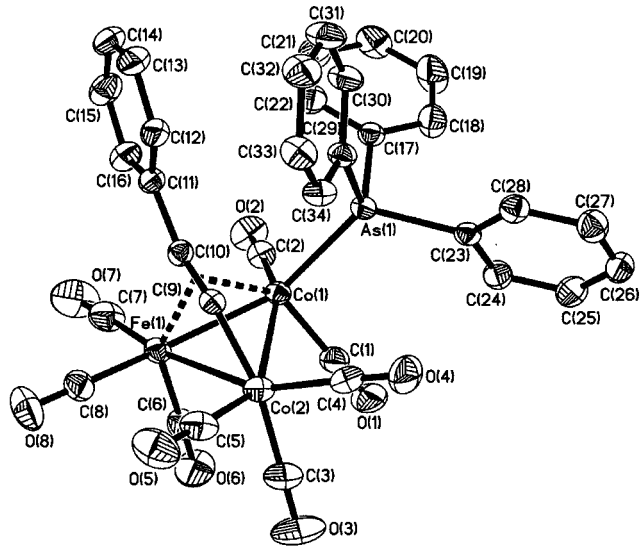


Fig. 3. Molecular structure of **4**.

Table 3
Selected bond lengths (Å) and bond angles (°) for **1**

| | | | |
|---|---|---|---|
| *Bond lengths* | | | |
| Co(1)–C(1) | 1.763(4) | C(9)–C(10) | 1.484(5) |
| Co(1)–C(8) | 1.859(3) | Co(2)–C(8) | 1.870(3) |
| Co(1)–P(2) | 2.2192(10) | Co(2)–P(1) | 2.2036(10) |
| Co(1)–C(9) | 3.0560(4) | Co(2)–C(9) | 2.974(4) |
| Co(1)–Co(2) | 2.4749(7) | Co(2)–Fe(1) | 2.5402(7) |
| Co(1)–Fe(1) | 2.5584(7) | Fe(1)–C(8) | 1.960(3) |
| C(8)–C(9) | 1.383(4) | Fe(1)–C(9) | 2.263(4) |
| *Bond angles* | | | |
| P(2)–Co(1)–Co(2) | 97.72(3) | C(16)–P(1)–Co(2) | 110.03(11) |
| P(2)–Co(1)–Fe(1) | 143.93(4) | C(16)–P(2)–Co(1) | 107.80(11) |
| Co(2)–Co(1)–Fe(1) | 60.595(19) | C(9)–C(8)–Co(1) | 140.6(3) |
| P(1)–Co(2)–Co(1) | 95.68(3) | C(9)–C(8)–Co(2) | 131.7(3) |
| P(1)–Co(2)–Fe(1) | 142.92(4) | Co(1)–C(8)–Co(2) | 83.18(14) |
| Co(1)–Co(2)–Fe(1) | 61.329(19) | C(8)–C(9)–C(10) | 128.6(4) |
| Co(2)–Fe(1)–Co(1) | 58.076(19) | P(1)–C(16)–P(2) | 109.76(17) |

Table 4
Selected bond lengths (Å) and bond angles (°) for **2**

| | | | |
|---|---|---|---|
| *Bond lengths* | | | |
| Co(1)–C(9) | 1.893(3) | Fe(1)–C(9) | 1.947(3) |
| Co(1)–P(1) | 2.2424(9) | Fe(1)–C(10) | 2.735(17) |
| Co(1)–Fe(1) | 2.5007(6) | C(1)–O(1) | 1.136(4) |
| Co(1)–Co(2) | 2.5094(6) | C(3)–O(3) | 1.126(4) |
| Co(2)–C(9) | 1.903(3) | C(9)–C(10) | 1.481(11) |
| Co(2)–Fe(1) | 2.4962(6) | C(10)–C(11) | 1.447(14) |
| *Bond angles* | | | |
| C(1)–Co(1)–Fe(1) | 94.14(11) | C(9)–Co(2)–Fe(1) | 50.36(9) |
| C(2)–Co(1)–Fe(1) | 99.76(12) | C(9)–Co(2)–Co(1) | 48.45(9) |
| C(9)–Co(1)–Fe(1) | 50.31(9) | Fe(1)–Co(2)–Co(1) | 59.943(17) |
| P(1)–Co(1)–Fe(1) | 158.76(3) | Co(2)–Fe(1)–Co(1) | 60.290(17) |
| C(9)–Co(1)–Co(2) | 48.79(9) | C(10)–C(9)–Co(1) | 134.2(6) |
| P(1)–Co(1)–Co(2) | 106.09(3) | C(10)–C(9)–Co(2) | 143.0(6) |
| Fe(1)–Co(1)–Co(2) | 59.767(17) | Co(1)–C(9)–Co(2) | 82.76(12) |

Table 5
Selected bond lengths (Å) and bond angles (°) for **4**

| | | | |
|---|---|---|---|
| *Bond lengths* | | | |
| Co(1)–C(9) | 1.995(3) | Co(2)–Fe(1) | 2.6115(7) |
| Co(1)–C(10) | 2.135(3) | Fe(1)–C(9) | 2.024(3) |
| Co(1)–As(1) | 2.4027(6) | Fe(1)–C(10) | 2.072(3) |
| Co(1)–Fe(1) | 2.4938(7) | C(1)–O(1) | 1.139(4) |
| Co(1)–Co(2) | 2.5962(7) | C(3)–O(3) | 1.129(4) |
| Co(2)–C(9) | 1.832(3) | C(9)–C(10) | 1.293(4) |
| *Bond angles* | | | |
| C(9)–Co(1)–Fe(1) | 52.18(9) | Co(1)–Co(2)–Fe(1) | 57.222(18) |
| As(1)–Co(1)–Fe(1) | 148.62(2) | C(9)–Fe(1)–Co(1) | 51.14(9) |
| C(9)–Co(1)–Co(2) | 44.70(9) | Co(1)–Fe(1)–Co(2) | 61.081(19) |
| As(1)–Co(1)–Co(2) | 107.02(2) | C(10)–C(9)–Co(2) | 155.3(3) |
| Fe(1)–Co(1)–Co(2) | 61.70(2) | C(10)–C(9)–Co(1) | 77.8(2) |
| C(9)–Co(2)–Co(1) | 50.00(10) | Co(2)–C(9)–Co(1) | 85.31(13) |
| C(9)–Co(2)–Fe(1) | 50.56(10) | C(9)–C(10)–Co(1) | 66.0(2) |

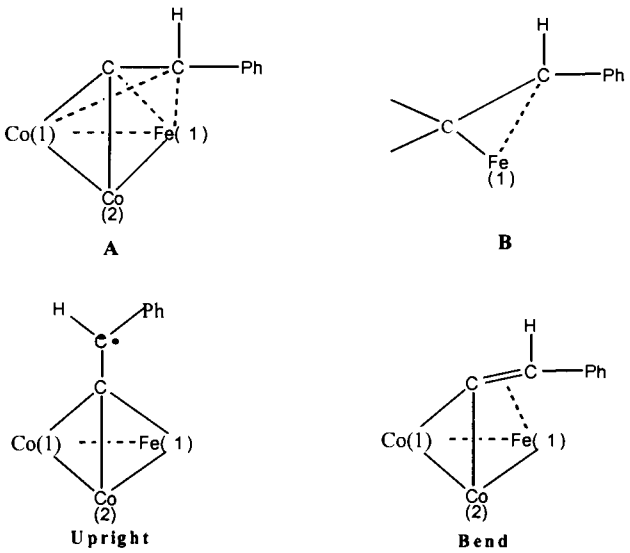


Scheme 3.

interaction between the vinylidene and the Co(1) atom with which C(β) atom is relatively weak in **4**. These facts clearly show that in **4** the bonding of the vinylidene to the Fe(1) and Co(1) atoms could be described as olefin–metal interaction, i.e. **A** (see Scheme 3) where the C(α) and C(β) atoms are both interacting strongly with Fe(1) and Co(1) atoms in a typical $\eta^2$-olefin/metal π-bond. The iron–carbon bond length data in **2** reveal that vinylidene is much more 'upright' type and C(β) atom is only weakly interacting with Fe(1) atom, i.e. **B** (see Scheme 3). The situation in **1** is closer to the 'bend' type [13]. The C=C bond lengths within the apical >C(α)=C(β)H(Ph) group in **2** (1.481 Å) and **1** (1.383 Å) are longer than that in the parent cluster **5** (1.31 Å) presumably because of the $\eta^2$-interaction between the vinylidene double bond and the Fe(1) atom. The C=C bond length in **4** (1.293 Å) is shorter than that in the parent cluster **5**, and this bond length is intermediate between a C=C double bond and a C≡C triple bond. The metal–carbon bond length data in **4** (Co(1)–C(α), 1.995 Å; Co(1)–C(β), 2.1353 Å; Co(2)–C(α), 1.832 Å; Fe(1)–C(α), 2.024 Å; Fe(1)–C(β), 2.072 Å) clearly demonstrate that the cobalt atoms Co(1) and Co(2) are more strongly bound to the C(α) atom than the unique iron atom Fe(1), but the Co(1) atom interacts more weakly with C(β) atom than the Fe(1) atom. The Co(1)–As(1) distance (2.4027 Å) in **4** is longer than the average Co–P bond length (2.238 Å) in **1** and **2** as expected from the different covalent radii of phosphorus (1.10 Å) and arsenic (1.21 Å). The dihedral angles data between C(α)–Co(1)–Co(2) and Fe(1)–Co(1)–Co(2) planes (60.4° for **1**, 61.8° for **2**) support the conclusion that in **1** the $\eta^2$-interaction between the vinylidene double bond and Fe(1) atom is stronger than in **2**, and in **4** a greater dihedral angle (63.5°) is the reason for an interaction between Co(1) and C(β) atoms. The geometry of the $FeCo_2$ core in **1** (Co(1)–Fe(1), 2.5584 Å; Co(2)–Fe(1), 2.5402 Å; Co(1)–Co(2), 2.4749 Å) is similar to that of the parent cluster **5** (Co(1)–Fe(1), 2.498 Å; Co(2)–Fe(1), 2.519 Å; Co(1)–Co(2), 2.473 Å). It may be seen that the geometry of the $FeCo_2$ core in **2** is close to that of an equilateral triangle from the corresponding bond lengths and angles [Co(1)–Fe(1), 2.5007 Å; Co(2)–Fe(1), 2.4962 Å; Co(1)–Co(2), 2.5094 Å. Fe(1)–Co(1)–Co(2), 59.767°; Fe(1)–Co(2)–Co(1), 59.943°; Co(2)–Fe(1)–Co(1), 60.290°]. The Co(2)–Fe(1) (2.6115 Å) and Co(1)–Co(2) (2.5962 Å) bonds in **4** are significantly elongated in comparison with the corresponding bond lengths of the parent cluster **5**. The data on bond angles in **1** [P(1)–Co(2)–Fe(1), 142.92° and P(2)–Co(1)–Fe(1), 143.93°], **2** [P(1)–Co(1)–Fe(1), 158.76° and P(1)–Co(1)–Co(2), 106.09°] and **4** [As(1)–Co(1)–Fe(1) 148.62° and As(1)–Co(1)–Co(2) 107.02°] show that dppm replaces two equatorial carbonyls from two $Co(CO)_3$ groups, and $PPh_3$ and $AsPh_3$ replace one equatorial carbonyl from $Co(CO)_3$ group, respectively. The new clusters **1**, **2** and **4** have 48 cluster valence electrons and hence obey the effective atomic number rule (3 M–M).

## 3. Experimental

### 3.1. General procedures

All reactions and manipulations were carried out using standard Schlenk techniques under an atmosphere of pure $N_2$. Solvents were purified, dried and distilled under a $N_2$ atmosphere prior to use. The reactions were monitored by TLC. Chromatographic separations and purification were performed on 200–300 mesh silica gel. The dppm, $PPh_3$ and $AsPh_3$ were purchased from Fluka. The starting material {$\mu_3$-

H(Ph)C=C}$FeCo_2(CO)_9$ [10] was prepared according to the literature method.

IR spectra were recorded on a Mattson Alpha-Centauri FT-IR spectrometer as KBr disks. Elemental analyses were carried out on a Carlo Erba 1106-type analyzer. $^1$H-NMR spectra in $CDCl_3$ were recorded using a Varian Mercury 300 MHz spectrometer. $^{31}$P-NMR spectra in $CH_2Cl_2$ were measured on a Bruker AC-200P FT-NMR instrument. The mass spectra were determined by using Hitachi M-80 GC/MS/DS and VG ZAB-HS instruments. Melting points (m.p.) were determined using XT-4 melting point apparatus.

### 3.2. Synthesis of {$\mu_3$-H(Ph)C=C}$FeCo_2(CO)_7$dppm (1)

A toluene solution of {$\mu_3$-H(Ph)C=C}$FeCo_2(CO)_9$ (100 mg, 0.189 mmol), dppm (70 mg, 0.182 mmol) and 8.5 mg $Me_3NO$ was stirred for 8 h at 75 °C. The solvent of the resulting dark-green mixture was removed under vacuum. The residue was dissolved in a minimal amount of $CHCl_3$ and was subjected to chromatographic separation on a silica gel column (2.0 × 40 cm). Elution with a mixture of hexane–benzene (1:1, v/v) afforded a dark-green band (**1**). Crystals of **1** were obtained by recrystallizing the solid **1** from hexane–$CH_2Cl_2$ at −20 °C. Yield, 33%; m.p., 181–182 °C. Anal. Found: C, 55.94; H, 3.43. Calc. for $C_{40}H_{28}Co_2FeO_7P_2$: C, 56.11; H, 3.30%. IR (KBr disk, $cm^{-1}$): $\nu$(CO) 2043vs, 1997vs, 1968s, 1961w, 1935m, 1912w. $^1$H-NMR ($CDCl_3$): $\delta = 7.45–7.03$ (m, 25H, $C_6H_5$), 6.92 (s, 1H, C–H), 3.40 (t, 2H, $J = 12.6$ Hz, $CH_2$). $^{31}$P-NMR ($CH_2Cl_2$): $\delta = 47.14$ (br, $PPh_3$). FDMS 856 [$M^+$].

### 3.3. Synthesis of {$\mu_3$-H(Ph)C=C}$FeCo_2(CO)_{9-n}L_n$ [L = PPh$_3$, n = 1 (2), 2 (3)]

A benzene solution of {$\mu_3$-H(Ph)C=C}$FeCo_2(CO)_9$ (100 mg, 0.189 mmol), $PPh_3$ (100 mg, 0.382 mmol) and 8.5 mg $Me_3NO$ was stirred for 12 h at 75 °C. The solvent of the resulting dark-green mixture was removed under vacuum. The residue was dissolved in a minimal amount of $CHCl_3$ and was subjected to chromatographic separation on a silica gel column (2.0 × 40 cm). Elution with a mixture of hexane–benzene (5:1, v/v) afforded a dark-green band (**2**). Further elution with a mixture of hexane–benzene (1:1, v/v) gave a dark-green band (**3**). Crystals of **2** were obtained by recrystallizing the solid **2** from hexane at −20 °C. Cluster **2**: Yield, 36%; m.p., 112–113 °C. Anal. Found: C, 53.66; H, 2.83. Calc. for $C_{34}H_{21}Co_2FeO_8P$; C, 53.58; H, 2.78%. IR (KBr disk, $cm^{-1}$): $\nu$(CO) 2069vs, 2027vs, 2006vs, 1988w, 1976w. $^1$H-NMR ($CDCl_3$): $\delta = 7.51–7.00$ (m, 20H, $C_6H_5$), 6.91 (s, 1H, C–H). $^{31}$P-NMR ($CH_2Cl_2$): $\delta = 50.02$ (br, $PPh_3$). FDMS: 762 [$M^+$]. Cluster **3**: Yield, 12%; m.p., 164–165 °C. Anal. Found: C, 61.25; H, 3.60. Calc. for $C_{51}H_{36}Co_2FeO_7P_2$: C, 61.47; H, 3.64. IR (KBr disk, $cm^{-1}$): $\nu$(CO) 2036s, 1995vs, 1981vs. $^1$H-NMR ($CDCl_3$): $\delta = 7.53–7.17$ (m, 35H, $C_6H_5$), 6.87 (s, 1H, C–H). $^{31}$P-NMR ($CH_2Cl_2$): $\delta =$ 50.02 (br, $PPh_3$). FABMS ($Cs^{133}$): 996 [$M^+$], 968 [$M^+ - CO$], 940 [$M^+ - 2CO$], 912 [$M^+ - 3CO$], 884 [$M^+ - 4CO$].

### 3.4. Synthesis of {$\mu_3$-H(Ph)C=C}$FeCo_2(CO)_8AsPh_3$ (4)

A benzene solution of {$\mu_3$-H(Ph)C=C}$FeCo_2(CO)_9$ (200 mg, 0.379 mmol), $AsPh_3$ (116 mg, 0.379 mmol) and 17 mg $Me_3NO$ was stirred for 24 h at 75 °C. The solvent of the resulting dark-green mixture was removed under vacuum. The residue was dissolved in a minimal amount of $CHCl_3$ and was subjected to chromatographic separation on a silica gel column (2.0 × 40 cm). Elution with a mixture of hexane–benzene (1:1, v/v) afforded a dark-green band (**4**). Crystals of **4** were obtained by recrystallizing the solid **4** from hexane at −20 °C. Cluster **4**: Yield, 23%; m.p., 113–114 °C. Anal. Found: C, 50.70; H, 2.64%. Calc. for $C_{34}H_{21}AsCo_2FeO_8$: C, 50.66; H, 2.63. IR (KBr disk, $cm^{-1}$): $\nu$(CO) 2070vs, 2017vs, 2012m, 1988w, 1966w, 1944w. $^1$H-NMR ($CDCl_3$): $\delta = 7.51–7.00$ (m, 20H, $C_6H_5$), 6.91 (s, 1H, C–H). FDMS: 806 [$M^+$].

### 3.5. X-ray crystallography of the new clusters 1, 2 and 4

The dark-green crystals of **1**, **2** and **4** (approximate dimensions 0.20 × 0.15 × 0.05 mm$^3$, 0.45 × 0.40 × 0.05 mm$^3$ and 0.45 × 0.30 × 0.25 mm$^3$, respectively) were mounted on a glass fiber. All measurements were made on a Bruker SMART 1000 CCD diffractometer with graphite monochromated Mo–$K_\alpha$ ($\lambda = 0.71073$ Å) radiation. All data were collected at 20 °C using the $\omega$ scan techniques. All structures were solved by direct methods and refined using Fourier techniques [19]. An absorption correction based on the SADABS was applied [20]. All non-hydrogen atoms were refined by the full-matrix least-squares on $F^2$. Hydrogen atoms were located and refined by the geometry method. The cell refinement, data collection and reduction were done by Bruker SAINT and SMART [21]. The structure solution and refinement were performed by SHELXSL-97 [22]. For further crystal data and details of measurements see Table 2.

## 4. Supplementary material

Crystallographic data for structural analysis have been deposited with the Cambridge Crystallographic Data Centre, CCDC nos. 160443–160445 for compounds **1**, **2** and **4**, respectively. Copies of this informa-

tion may be obtained free of charge from The Director, CCDC, 12 Union Road, Cambridge CB2 1EZ, UK (Fax: +44-1223-336033; e-mail: deposit@ccdc.cam.ac.uk or www: http://www.ccdc.cam.ac.uk).

## Acknowledgements

We are grateful to the Inner Mongolia Science Foundation for financial support of this work.

## References

[1] H. Vahrenkamp, Adv. Organomet. Chem. 22 (1983) 169.
[2] F.G.A. Stone, M.L. Willioms, J. Chem. Soc. Dalton Trans. (1988) 2467.
[3] M.L. Ziegler, H.P. Neumann, Chem. Ber. 122 (1989) 25.
[4] E. Sappa, A. Tiripicchio, P. Braunstein, Chem. Rev. 83 (1983) 203.
[5] E. Sappa, A. Tiripicchio, P. Braunstein, Coord. Chem. Rev. 65 (1985) 219.
[6] G. Davey, F.S. Stephens, J. Chem. Soc. Dalton Trans. (1974) 698.
[7] R. Rossetti, G. Gervasio, J. Chem. Soc. Dalton Trans. (1978) 222.
[8] S. Aime, L. Milone, R. Rossetti, Inorg. Chim. Acta 25 (1977) 103.
[9] P. Braunstein, L. Mourey, J. Rose, Organometallics 11 (1992) 2628.
[10] T. Albiez, W. Bernhardt, C. Schnering, E. Roland, H. Bantel, H. Vahrenkamp, Chem. Ber. 120 (1987) 141.
[11] H. Bantel, W. Bernhardt, A.K. Powell, H. Vahrenkamp, Chem. Ber. 121 (1988) 1247.
[12] S. Onaka, Y. Katsukawa, H. Furuta, J. Coord. Chem. 42 (1997) 77.
[13] M.F. D'Agostino, M. Mlekuz, J.W. Kolis, B.G. Sayer, C.A. Rodger, J.F. Halet, J.Y. Saillard, M.J. McGlinchey, Organometallics 5 (1986) 2345.
[14] P. Braunstein, J. Rose, D. Toussaint, Organometallics 13 (1994) 2472.
[15] S.B. Colbran, B.H. Robinson, J. Simpson, Organometallics 2 (1983) 952.
[16] (a) S.B. Colbran, B.H. Robinson, J. Simpson, Organometallics 2 (1983) 943;
(b) A.M. Bond, B.M. Peake, B.H. Robinson, J. Simpson, D.J. Watson, Inorg. Chem. 16 (1977) 410.
[17] K. Hinklemann, J. Heinze, H.T. Schacht, J.S. Field, H. Vahrenkamp, J. Am. Chem. Soc. 111 (1989) 5078.
[18] C.M. Arewgoda, B.H. Robinson, J. Simpson, J. Am. Chem. Soc. 105 (1983) 1893.
[19] G.M. Sheldrick, Acta Crystallogr. A 46 (1990) 467.
[20] G.M. Sheldrick, SADABS, Siemens Area Detector Absorption, Correction Software, University of Göttingen, Göttingen, Germany, 1996.
[21] SMART and SAINT, Area Detector Control and Integration Software, Bruker Analytical X-ray Instruments Inc., Madison, WI, USA, 1998.
[22] SHELXTL, Bruker Analytical X-ray Instruments Inc., Madison, WI, USA, 1998.